Report

2010 Annual WAMIT Consortium Meeting

November 9-10, 2010

Woods Hole, Massachusetts

Agenda for 2010 Annual WAMIT Meeting
Room 310, Marine Resource Center, Swope Center, Woods Hole, MA

November 9, 2010:

9:00AM: Welcome

9:20AM: "WAMIT V6.4 updates and Status of V6.4S"
C.-H. Lee, WAMIT

10:00AM: "Update on WAMIT Version 6.5"
J. N. Newman, WAMIT

10:30AM: "OpenMP in WAMIT"
X. Zhu, WAMIT

11:00AM: Break

11:20PM: "Making WAMIT models from solid models and IGES transfers"
R. Page, AeroHydro Inc.

12:00PM: Lunch, Swope Center Dining Hall

1:30 PM: "Wave Run-up and Air Gap Prediction for a Large-Volume Semi-Submersible Platform"
J. Sparano, The University of Sao Paulo

2:10PM: "Grue/Palm approach for the small current problem"
C.-H. Lee, WAMIT

3:00 PM: Break

3:30 PM: "Technical discussion"

5:30PM: Mixer and Dinner, Swope Center Dining Hall

November 10, 2009

9:00AM: “Technical discussion”

10:30AM: Break

11:00AM: Business meeting

12:00AM: Lunch, Swope Center Dining Hall

MultiSurf Training starts in the afternoon

Updates on V6.4

- V6.417: Error correction. When body pressure evaluated at user specified points (in .BPI), WAMIT fails to find the correct body surface points except the points on the first body.

- V6.416: Error correction. When ILOWHI=0, the mean forces using control surface may not be accurate, if IOPTN(7) >0 not specified.

- V6.415: Error correction. The vertical fluid velocity due to dipoles may not be accurate when the distance between the dipole and the field point is larger than the water depth. In the shallow water, the mean forces using control surface (see subsequent pages) and dipole elements may be affected.

Ellipsoid length 280m, beam 22m, and draft 11m, water depth 20m

	FIELD POINT AT X=150m Y= 0m			FIELD POINT AT X=120m Y= -6m		
PERIOD (Sec)	Vz_old	Vz_new	Difference	Vz_old	Vz_new	Difference
5.00	0.134292	0.134864	-0.000572	0.000496	0.000815	-0.000318
7.00	0.090586	0.090625	-0.000039	0.005446	0.004404	0.001042
9.00	0.056936	0.056840	0.000096	0.006232	0.005268	0.000964
11.00	0.037657	0.037572	0.000086	0.007966	0.007007	0.000959
13.00	0.026418	0.026335	0.000082	0.004608	0.003787	0.000822
15.00	0.020067	0.020000	0.000067	0.005300	0.004823	0.000477

Comparison of momentum, pressure and control surface drift force
(Ellipsoidal Control Surface 300m, 30m and 15m)

OLD CODE:	.8	.9	.9c	(.8-.9)	(.8-.9c)
5.00	3.586164	3.501611	3.679273	0.084553	0.093109
7.00	4.997672	4.988249	5.022538	0.009423	0.024866
9.00	5.936611	5.931874	5.583532	0.004737	0.353079
11.00	6.680754	6.677669	5.771374	0.003085	0.909380
13.00	6.194096	6.192014	4.593664	0.002082	1.600432
15.00	5.981401	5.980001	4.489932	0.001400	1.491469

NEW CODE:	.8	.9	.9c	(.8-.9)	(.8-.9c)
5.00	3.586164	3.501611	3.588301	0.084553	0.002137
7.00	4.997672	4.988249	4.997813	0.009423	0.000141
9.00	5.936611	5.931874	5.936776	0.004737	0.000165
11.00	6.680754	6.677669	6.680738	0.003085	0.000016
13.00	6.194096	6.192014	6.193794	0.002082	0.000302
15.00	5.981401	5.980001	5.981028	0.001400	0.000373

It was suggested to use control surfaces extended to the bottom of the shallow water at the meeting in 2009. This is unnecessary in V6.415 and later.

Status of WAMIT V6.4S

The new features in V6.4S

- Quadratic forces using control surfaces (Completed for both ILOWHI=0 and ILOWHI=1)
- Complete second-order forces on vessels with internal tanks (Completed for ILOWHI=0)
- Quadrature of the forcing over exact surface for ILOWHI=1

A computational example:a barge with two internal tanks.

Length 150m
Beam 50m
Draft 10m

Tank size 40mx40mx8m

Water depth 40m

Beam Sea

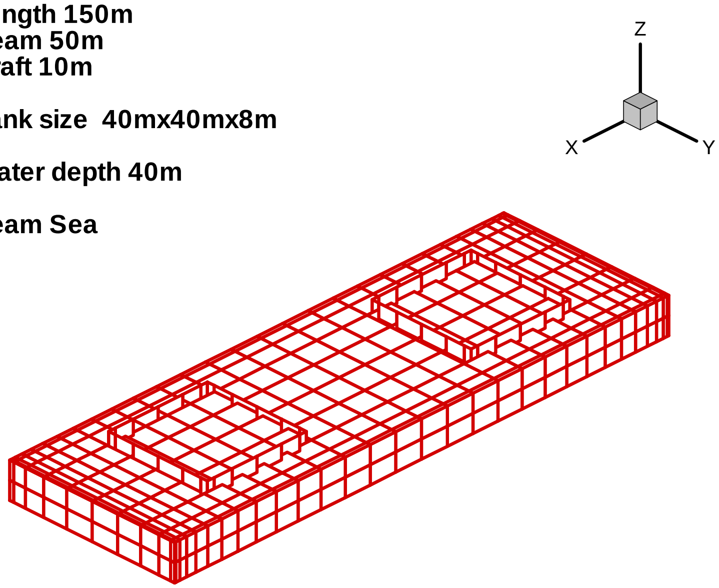

Average panel size is around 5m.

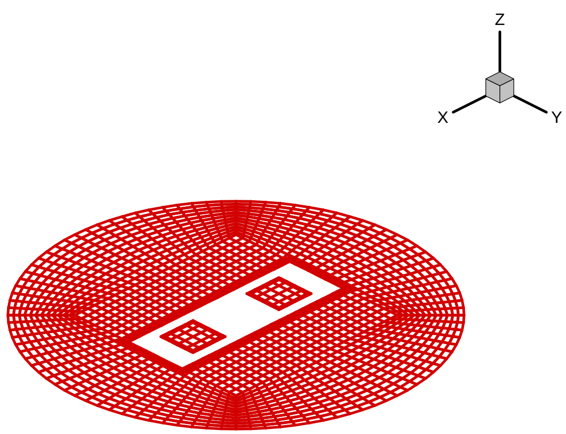

Average panel size is about 6m
Discretization extends to R=150m

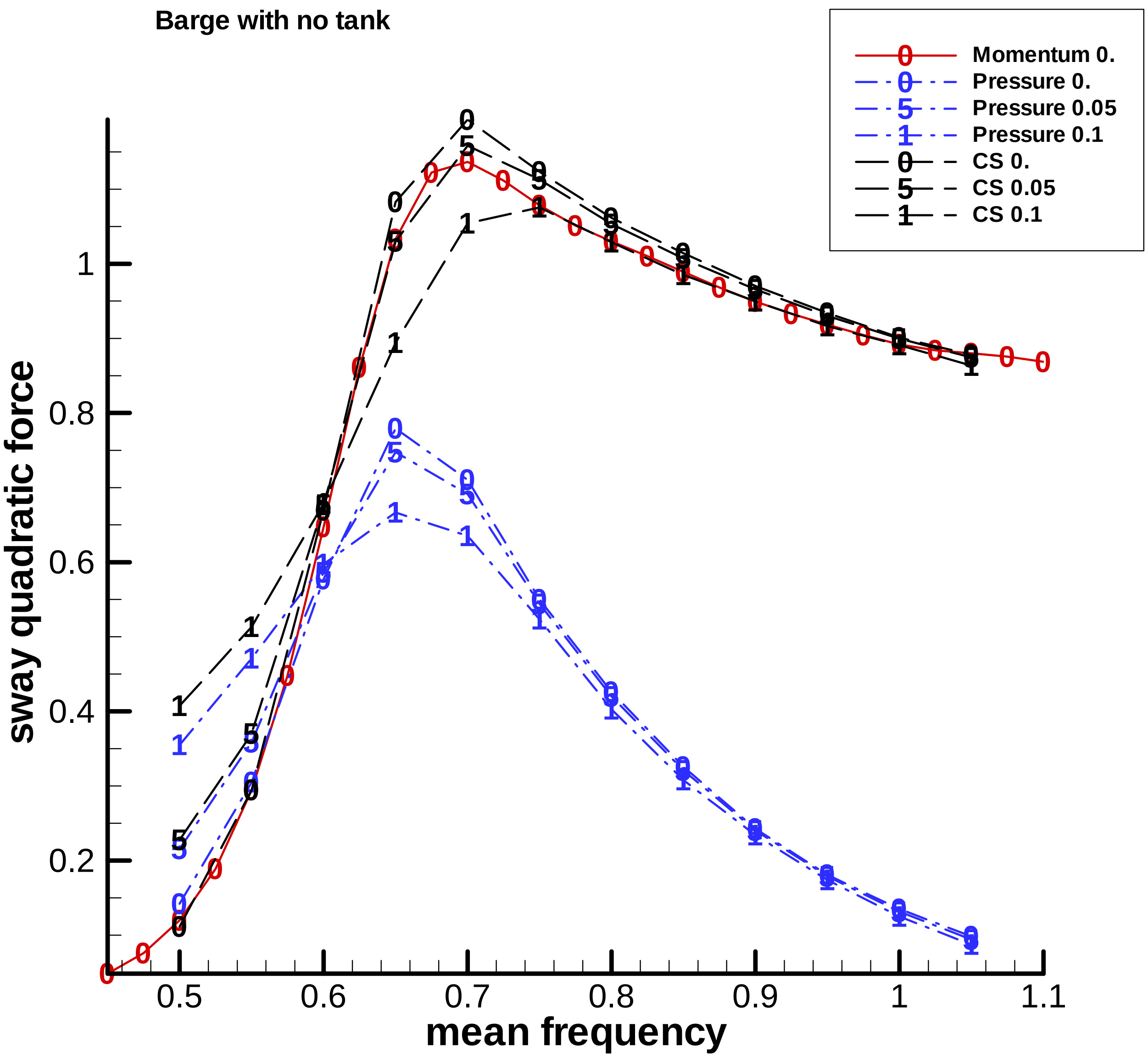

Barge with no tank
Momentum 0.
Pressure 0.
Pressure 0.05
Pressure 0.1
CS 0.
CS 0.05
CS 0.1
sway quadratic force
mean frequency
0.2
0.4
0.6
0.8
1
0.5
0.6
0.7
0.8
0.9
1
1.1

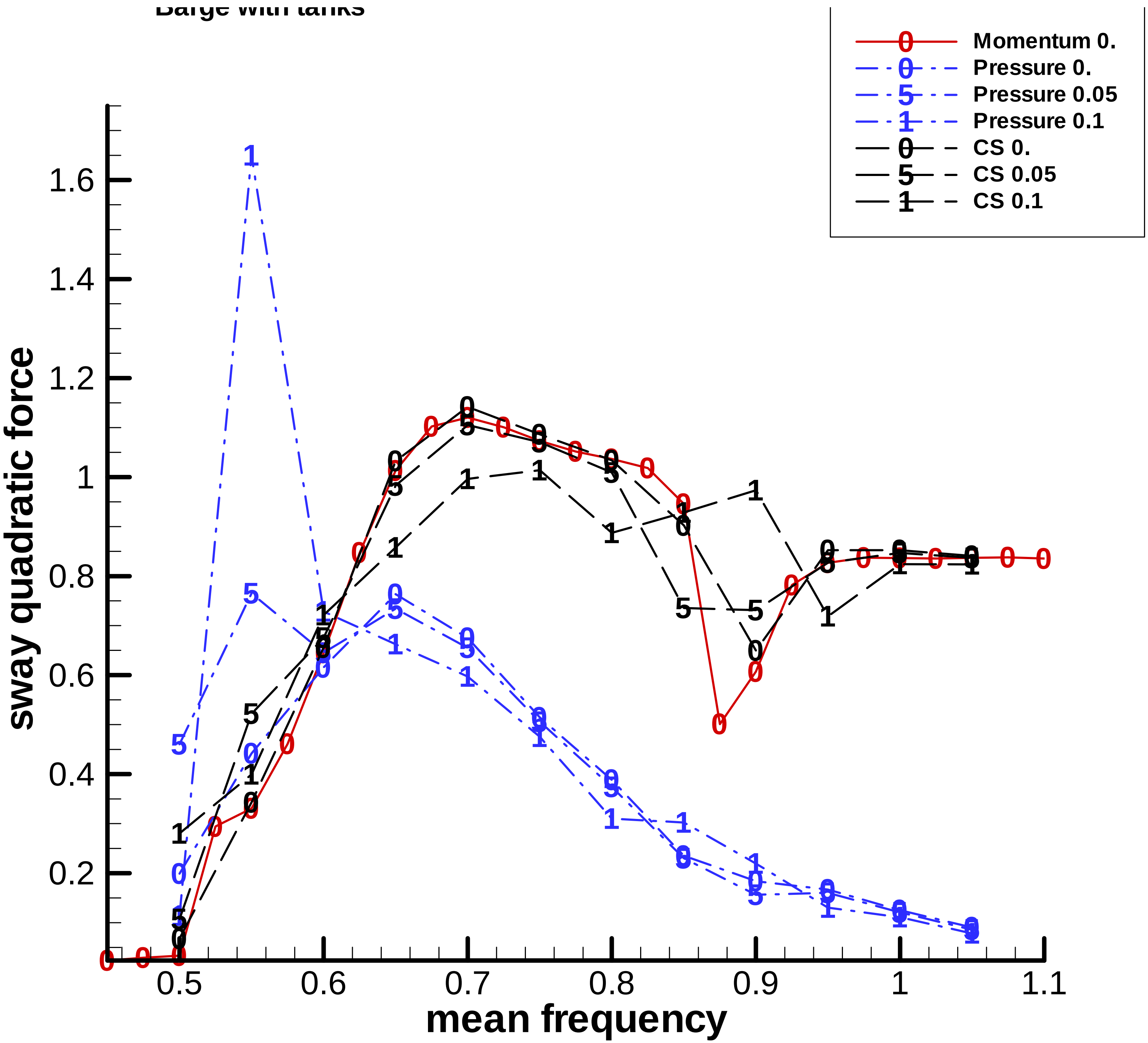

Barge with tanks
Momentum 0.
Pressure 0.
Pressure 0.05
Pressure 0.1
CS 0.
CS 0.05
CS 0.1
sway quadratic force
mean frequency
1.6
1.4
1.2
1
0.8
0.6
0.4
0.2
0.5
0.6
0.7
0.8
0.9
1
1.1

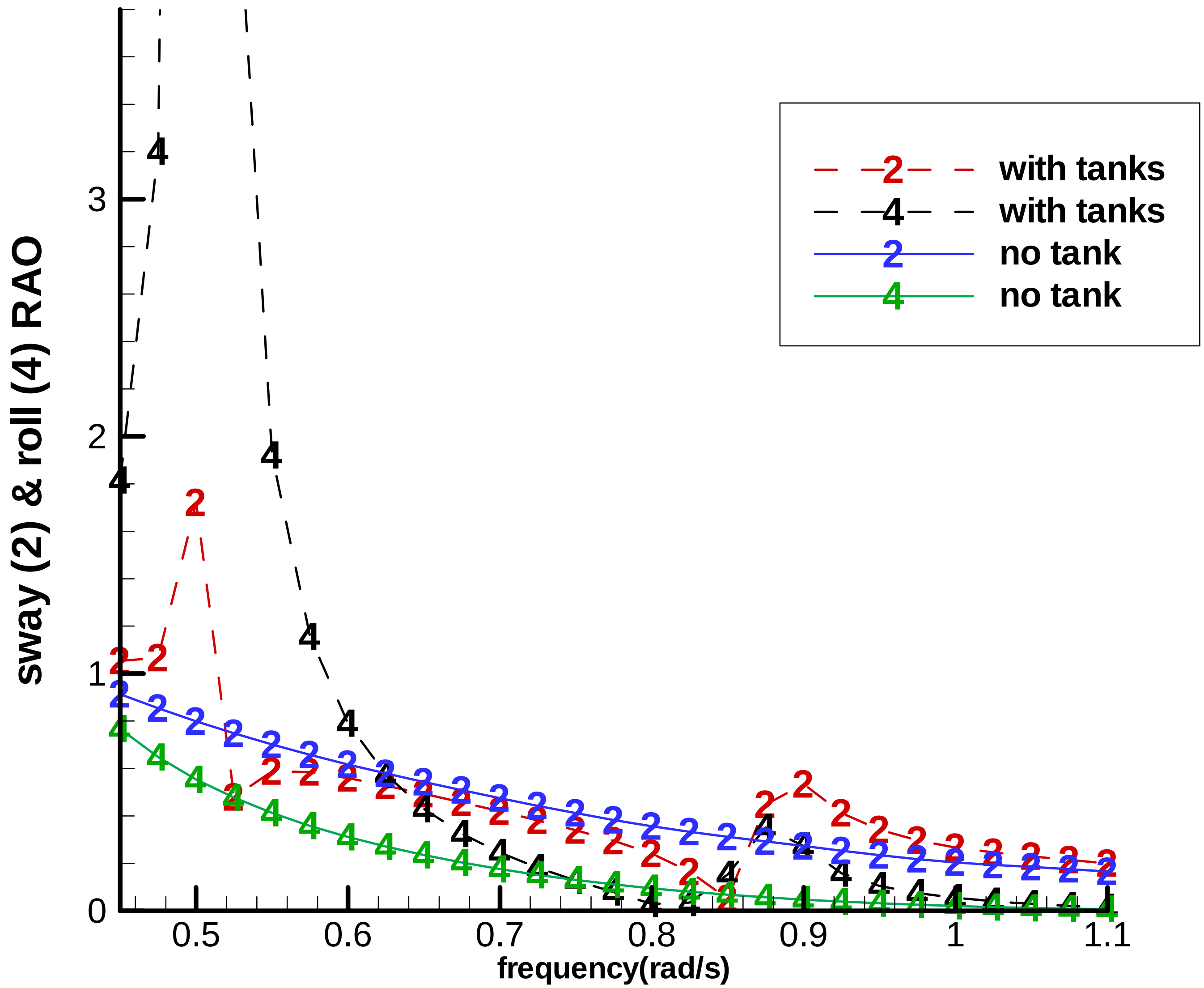

sway (2) & roll (4) RAO
frequency(rad/s)
0
1
2
3
0.5
0.6
0.7
0.8
0.9
1
1.1
2 with tanks
4 with tanks
2 no tank
4 no tank

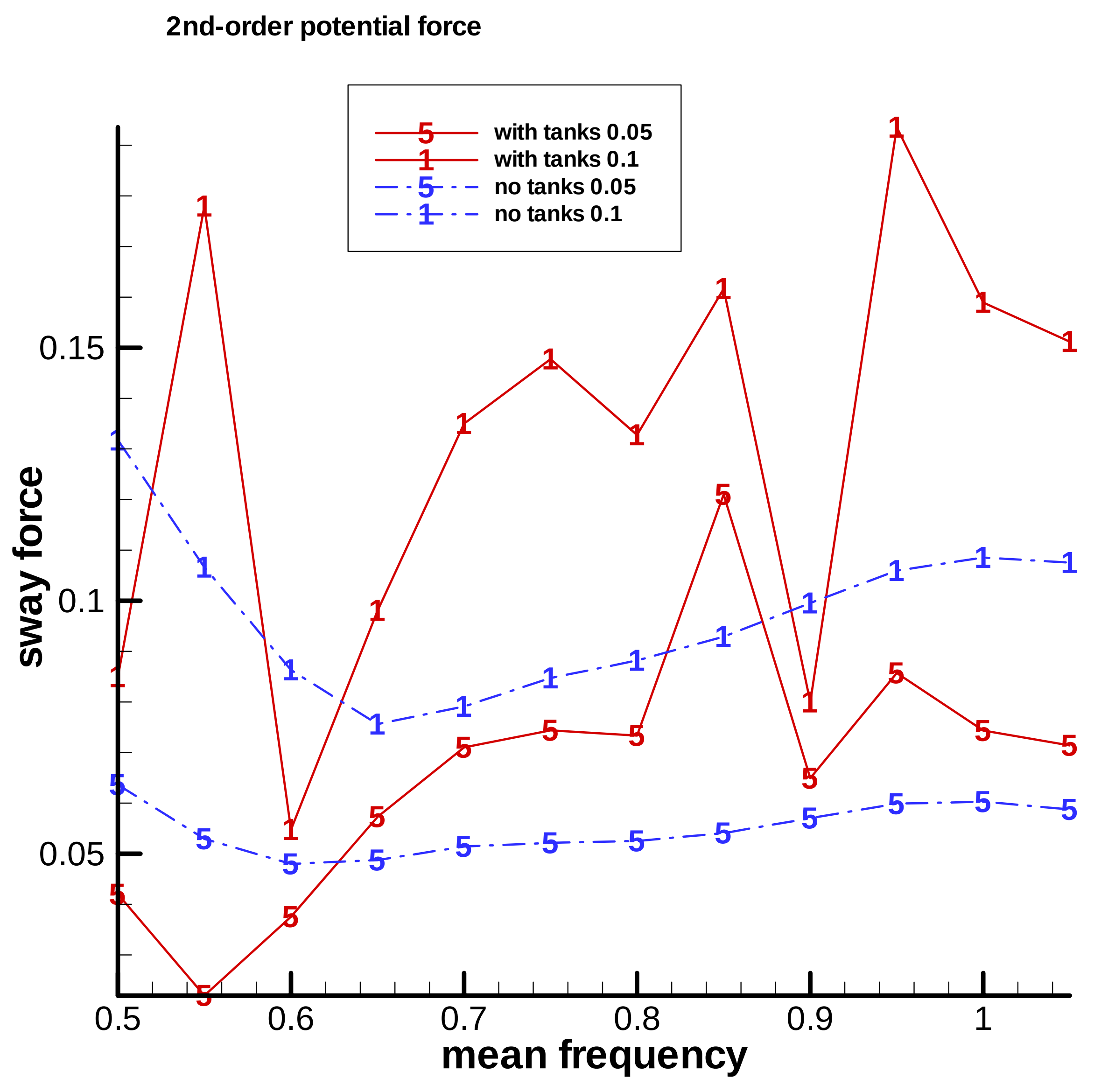
2nd-order potential force
with tanks 0.05
with tanks 0.1
no tanks 0.05
no tanks 0.1
sway force
0.15
0.1
0.05
0.5
0.6
0.7
0.8
0.9
1
mean frequency

- Extension is made to calculate the quadratic forces using control surface. A computational example based on the low order method shows this approach is significantly more accurate than the direct pressure integral for the difference frequency forces.

- For ILOWHI=0, extension is made to account the complete 2^{nd}-order effect in the internal tanks.

Update on WAMIT Version 6.5

List of proposed extensions

October 2009

- Option to exploit geometric symmetry when NBODY>1
- Output patch data in header of .out file if NPER=0
- Improved error messages for bad input files
- ~~Option to interrupt/restart run and save Rankine data~~
- ~~Option to run new frequencies with saved Rankine data~~
- Grue & Palm small velocity/current interaction

Additional extensions
November 2010

- Evaluate option 9c (control surface drift forces) without option 9 (pressure integration on body surface)
- For option 9, list points with velocity > VMAXOPT9
- Modify tolerance for gaps on waterline
- Evaluate separate Froude-Krylov and scattering components of exciting force
- Use both **`config.wam`** and **`runid.cfg`** files for input
- New algorithms for Rankine and Log singularities in the low-order method
- Use RAMGBMAX to avoid scratch disk I/O
- IFORCE=2: evaluate FORCE outputs in POTEN period loop
- OpenMP !

OpenMP in WAMIT

OpenMP in WAMIT Flow Chart

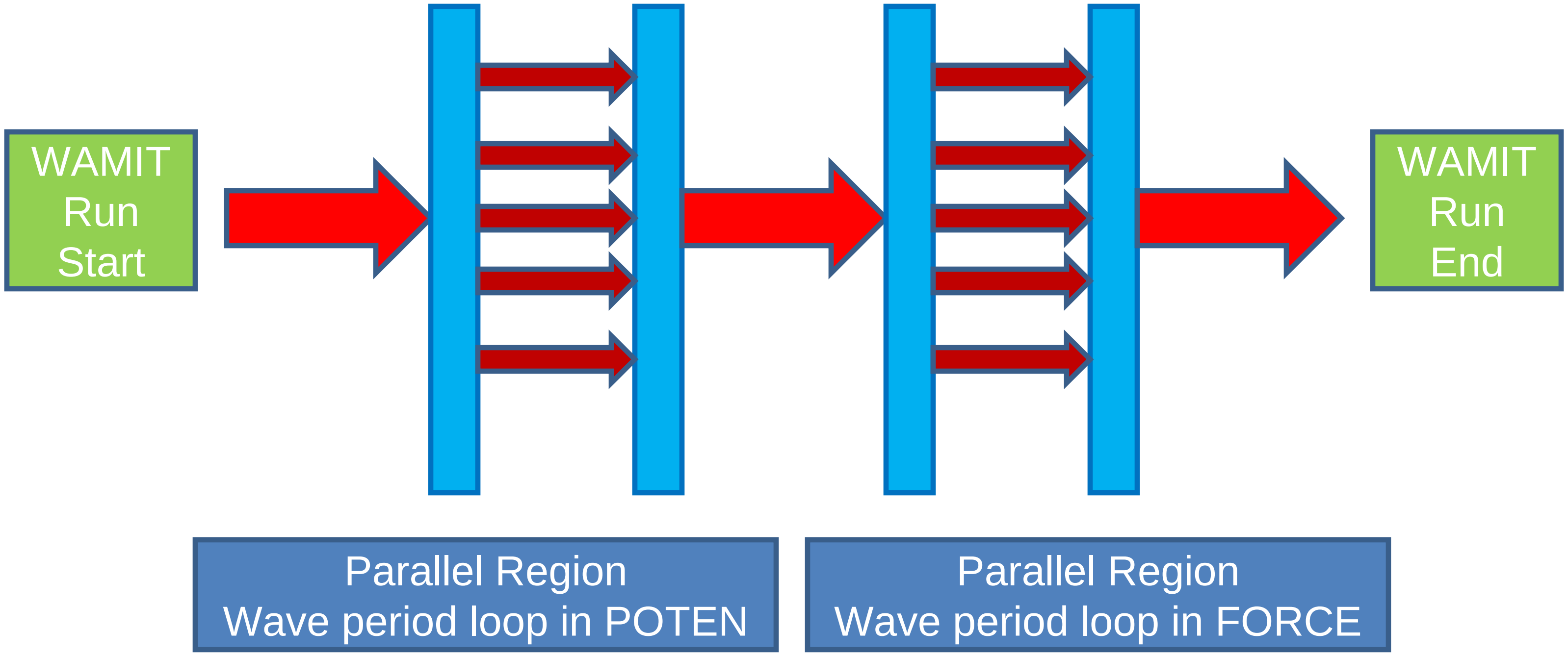

- Parallel region to cover as much as code as possible to improve performance.
- WAVEGR, SOLVE, MDRFTP are parallelized. RANKIN is not.
- Combined into one parallel region if IFORCE=2.

OpenMP Technical Challenges

- Scratch file I/O problem
  - ❑ Run time library does heavy synchronization in reading from and writing to files. The original WAMIT V64 with OpenMP runs slower.
  - ❑ Use RAMGBMAX to avoid scratch disk I/O .
- Data dependence problem
  - ❑ Add wave period number or thread number index to LHS arrays, RHS arrays , and FORCE output arrays. More RAM required for the same WAMIT run.
  - ❑ Some changes inside code, mainly arrays allocation, to remove data dependence problem.
  - ❑ Still in the middle of debugging. Some bugs are hard to find.

Estimated RAM Space Required

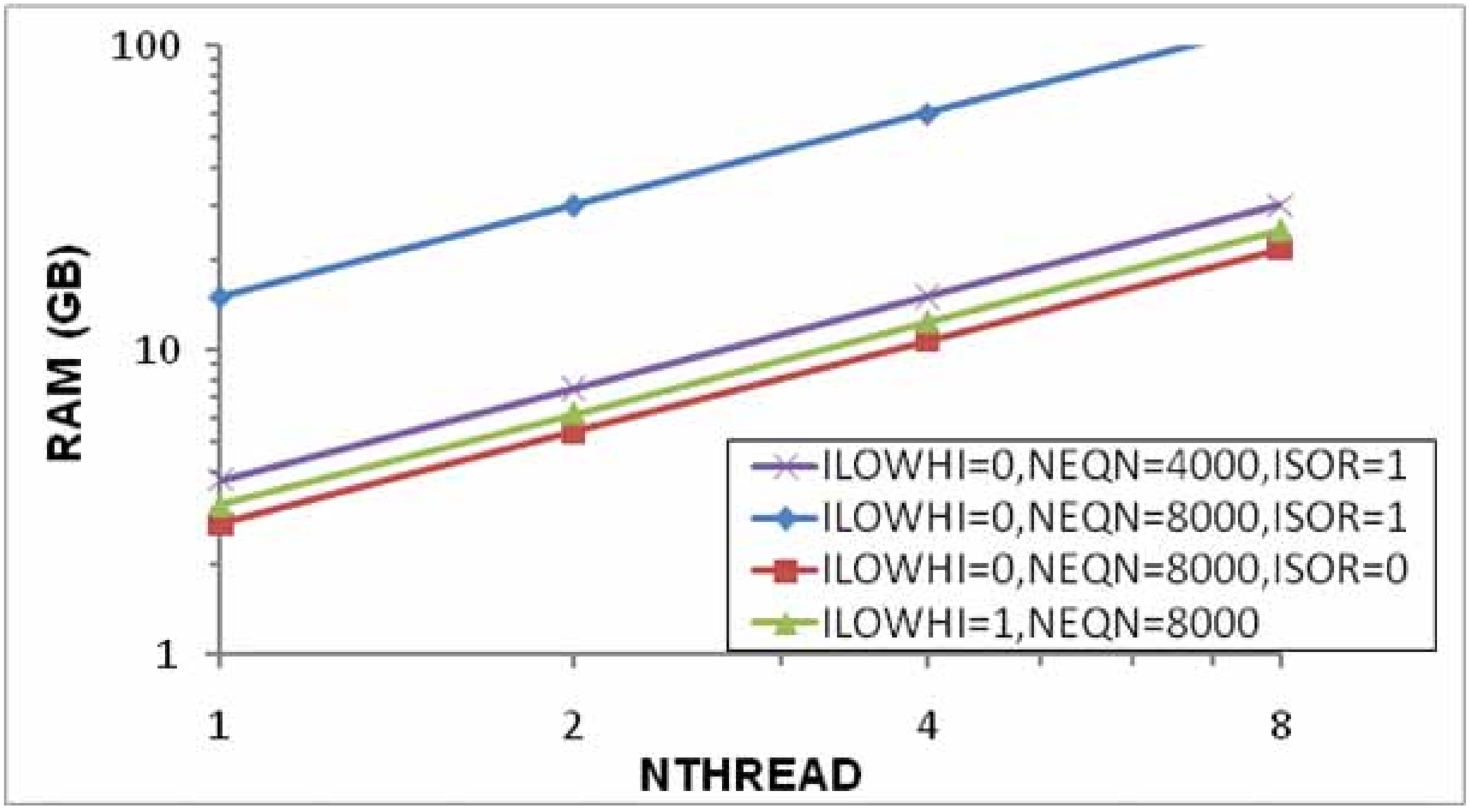

- NLHS=4, ILOG=0

Timing tests for speedup of parallel code
(variants of TEST07 and TEST15)

- Test system: Dell T7500 (August 2010)
- OS: Windows XP Pro 64-bit (x64)
- dual quad-core (8 cpu’s) 2.26GHz
- RAM: 96 GB (up to 192 GB is possible)

Details of test runs:

IFORCE=2, RAMGBMAX=90.0, and other changes from standard test runs denoted in red.

- test07: (ISSC TLP, low-order, NPER=64, NEQN=1012 and 4048, NLHS=2, ISOR=1, ILOG=1)
- test15: (Semi-sub, higher-order, NPER=16, NEQN=314, ISOLVE=1, ILOG=0, includes control-surface drift force option 9c)

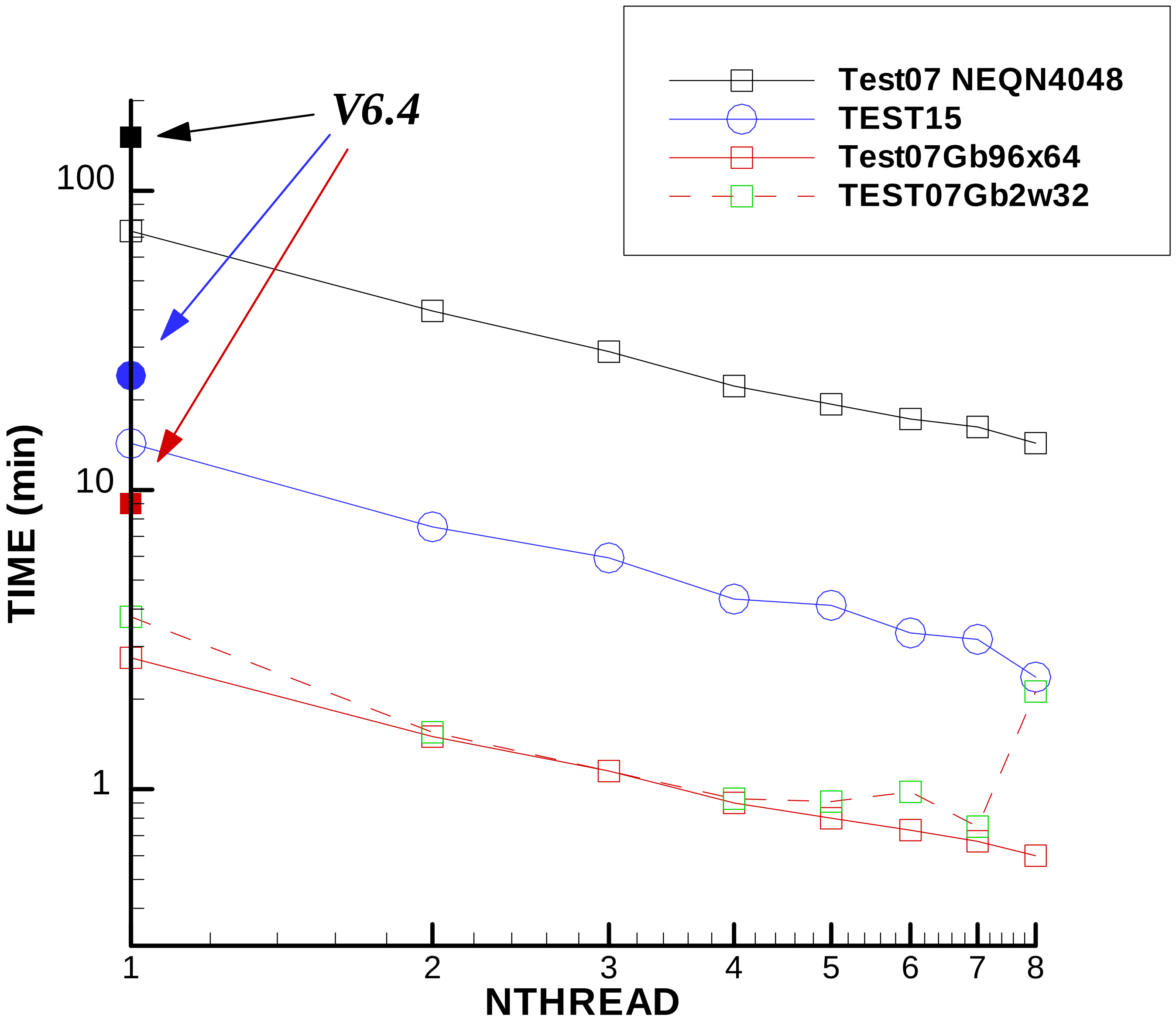
V6.4
Test07 NEQN4048
TEST15
Test07Gb96x64
TEST07Gb2w32
100
10
1
TIME (min)
1
2
3
4
5
6
7
8
NTHREAD

Conclusions

- OpenMP shows promising results to reduce the computational time.
- Larger RAM is required for WAMIT with multiple threads compared to that of V64.
- Still in debugging mode for WAMIT.

Outline of Grue/Palm approach for the small current problem

Following Nossen et al (1991), Grue & Biberg (1993) and Grue & Palm (1993), the total velocity potential, in the presence of current, is written in the form

$$\Phi = \phi_s(x) + \Phi^1(x,t) + \psi^2(x) + ...$$

ϕ_s denotes the potential due to the current and the steady flow, Φ^1 the linear time harmonic potential and ψ^2 the second-order steady potential. The positive current direction is assumed toward the negative x direction (or the positive forward speed is toward the positive x).

1 Steady Potential

The steady potential may be decomposed into the uniform current and steady disturbance due to the body.

$$\phi_s = U\chi_s = U(\chi - x)$$

To leading order in U, the steady potential satifies

$$\frac{\partial \chi}{\partial z} = 0 \quad \text{on} \quad z = 0$$

and on the body

$$\frac{\partial \chi}{\partial n} = n_1 \quad \text{on} \quad z = 0$$

(χ is the same when current changes direction to -U, regardless of the body symmetry in x.)

2 Linear Potential

The linear potential $\Phi^1(x,t)$ may be decomposed into the incident, scattered and radition potentials

$$\Phi^1(x,t) = Re[(\phi_D(x) + \phi_R(x))e^{i\sigma t}] = Re[(\phi_I + \phi_S + i\sigma \sum_j \xi_j \phi_j e^{\imath\sigma t}]$$

The linear incident wave potential is

$$\phi_I = \frac{igA}{\omega} Z(z) e^{-i\nu'(x\cos\beta + y\sin\beta)}$$

where

$$Z(z) = \frac{\cosh[\nu'(z+h)]}{\cosh\nu' h}$$

which will be $e^{K'z}$ in the case of infinite depth.

2.1 Notations and normalization convention

The following notations are used in this note.

ω: incoming wave orbital frequency

$K' = \omega^2/g$: zero speed infinite depth wavenumber

ν' from $K' = \nu' \tanh(\nu' h)$: zero speed finite depth wavenumber

$\sigma = \omega - U\nu' cos\beta$: encounter frequency

$K = \sigma^2/g$

ν_0 from $K = \nu_0 \tanh(\nu_0 h)$

$\nu(\theta) = \nu_0(1 + 2\tau/C_g \cos\theta)$

$C_g(\nu' h) = [\tanh(\nu' h) + (\nu' h/\cosh^2(\nu' h))]$

$\tau = U\sigma/g$

$Fr = U/\sqrt{gL}$

When $U = 0$, $K' = K$, $\nu' = \nu_0 = \nu$

The steay and linear potentials are normalized in the following.

$\phi_s = \bar{\phi}_s(UL)$

$\chi_s = \bar{\chi}_s L = (\bar{\chi} - 1)L$

$\phi^1 = \bar{\phi}^1(\mathrm{i}\omega A/\sigma)$

$\bar{\phi}^1 = \bar{\phi}_I + \bar{\phi}_S + \mathrm{i}\bar{K}\sum_j \bar{\xi}_j \bar{\phi}_j$

$\bar{\phi}_I = \sqrt{K/K'} Z(z) e^{-i\nu'(x\cos\beta + y\sin\beta)}$

Normalization of other quantities follow the convention of WAMIT with the replacement of ω,K' or ν' with σ,K or ν.

2.2 Diffaction, Scattered and Radiation Potentials

The diffraction and raditaion potentials statisfy the free surface condition

$$-K\phi + 2i\tau\nabla_2\phi \cdot \nabla_2\chi_s + i\tau\nabla_2^2\chi_s + \frac{\partial\phi}{\partial z} = 0 \quad \text{on} \quad z = 0$$

The raditaion and scattering are subject to the body boundary condition

$$\frac{\partial \phi}{\partial n} = n_j + U/(i\sigma)m_j$$

where $(n_4, n_5, n_6) = x \times n$, $(m_1, m_2, m_3) = -n \cdot \nabla(\nabla \chi_s)$ and $(m_4, m_5, m_6) = -n \cdot \nabla(x \times \nabla \chi_s)$ and

$$\frac{\partial \phi}{\partial n} = -\frac{\partial \phi_I}{\partial n}$$

The linear potential is expanded in the speed parameter τ

$$\phi = \phi^0 + \tau \phi^1 + O(\tau^2)$$

2.3 Green function

The Green function is subject to the far field form of the free surface condition for ϕ

$$-KG - 2i\tau \nabla_2 G + \frac{\partial G}{\partial z} = 0 \quad \text{on} \quad z = 0$$

The Green function is expanded in the form

$$G = G^0 + \tau G^1 + O(\tau^2)$$

G^0 is the zero speed Green function of the frequency $\sigma(\omega, U, \beta)$ which may be written in the form

$$G^0 = \frac{1}{r} + \frac{1}{r'} + \frac{1}{r''} - 2K \log(K(r' + |z + \zeta|)) + H$$

$$G^1 = 2\mathrm{i}\frac{\partial}{\partial x}(\frac{\partial G^0}{\partial K}) = 2\mathrm{i}\frac{\partial}{\partial x}[-2\log(r' + |z + \zeta|) + \frac{\partial H}{\partial K}]$$

where $K = \sigma^2/g$. (For $\partial G^0/\partial K$, the log part $-2(1 + \log(K(r' + |z + \zeta|))$ should be added to $\partial H/\partial K$ when IFS=3.

(VGRN10 outputs G^0/K and its spacial derivatives in FV array and $\partial G^0/\partial K$ in DFV. Thus it should be noted $G^0 = K*$ FV and $\partial G^0/\partial K =$ DFV. Numerical differentiation is used to have G^0/K. The preliminary test indicates 3 to 4 significant digits accuracy over wide range of K and water depth.)

2.4 Integral Equations

ϕ^1 can be obtained as the solution of the integral equation given in the form

$$2\pi\phi_j^0 + \iint_{S_b} \phi_j^0 G_n^0 dS = \iint_{S_b} G^0 n_j dS$$

$$2\pi\phi_D^0 + \iint_{S_b} \phi_D^0 G_n^0 dS = 4\pi\phi_0$$

$$2\pi\phi_j^1 + \iint_{S_b} \phi_j^1 G_n^0 dS = \iint_{S_b} G^1 n_j - \phi_j^0 G_n^1 dS$$

$$-\frac{1}{i\nu}\iint_{S_b} \nabla G^0 \cdot (\nabla\chi - \hat{\imath}) n_j dS + i \iint_{S_f} \phi_j^0 (2\nabla_2 G^0 \cdot \nabla_2\chi + G^0 \nabla_2 \cdot \nabla_2 \chi) dS$$

$$2\pi\phi_D^1 + \iint_{S_b} \phi_D^1 G_n^0 dS = \iint_{S_b} -\phi_D^0 G_n^1 dS + i \iint_{S_f} \phi_D^0 (2\nabla_2 G^0 \cdot \nabla_2\chi + G^0 \nabla_2 \cdot \nabla_2 \chi) dS$$

The following relation may be used for the integrals involving $\nabla_2 \cdot \nabla_2 \chi$

$$\iint_{S_f} \phi G^0 \nabla_2 \cdot \nabla_2 \chi dS = -\int_{C_b} \phi G^0 n_1 dl - \iint_{S_f} (\nabla_2\phi \cdot \nabla_2\chi) G^0 + (\nabla_2 G^0 \cdot \nabla_2 \chi)\phi dS$$

3 Hydrodynamic coefficients, exciting forces and mean forces

The added mass and damping coeffcients are obtained from

$$a_{ij} - \frac{\mathrm{i}}{\sigma} b_{ij} = \rho \iint_{S_b} \{\phi_j - \frac{\mathrm{i}}{\sigma}[\nabla\phi_s \cdot \nabla\phi_j]\} n_i dS$$

or

$$\bar{a}_{ij} - \frac{\mathrm{i}}{\sigma}\bar{b}_{ij} = \iint_{S_b} \{\bar{\phi}_j - \mathrm{i}\frac{Fr}{\bar{K}}[(\nabla\bar{\chi} - \hat{\imath}) * \nabla\bar{\phi}_j]\} n_i dS$$

and the exciting force from

$$X_i = -\mathrm{i}\rho \iint_{S_b} (\mathrm{i}\sigma)\{\phi_D + [\nabla\phi_s \cdot \nabla\phi_D]\} n_i dS$$

or

$$\bar{X}_i = \iint_{S_b} \{\bar{\phi}_D - \mathrm{i}\frac{Fr}{\bar{K}}[(\nabla\bar{\chi} - \hat{\imath}) * \nabla\bar{\phi}_D]\} n_i dS$$

The horizontal mean forces and the vetical moment are obtained from the expressions

$$F_x = \rho g \frac{\nu_0}{4K'} \int_0^{2\pi} [C_g(\nu(\theta)h)\cos(\theta) + 2\tau \sin^2\theta] |H(\theta)|^2 d\theta + 2AC_g(\nu' h)\cos\beta Re[S]$$

$$F_y = \rho g \frac{\nu_0}{4K'} \int_0^{2\pi} [C_g(\nu(\theta)h)\sin(\theta) - 2\tau \sin\theta\cos\theta]|H(\theta)|^2 d\theta + 2AC_g(\nu'h)\sin\beta Re[S]$$

$$M_z = \frac{\rho g}{4K'} \int_0^{2\pi} [(C_g(\nu(\theta)h) - 2\tau\cos(\theta)]Im[H(H^*)']d\theta$$

$$-\frac{\rho g}{2K'}\{(1 - \frac{\nu'}{C_g(\nu'h)}\frac{dC_g(\nu'h)}{d\nu'})\tau\sin\beta Im[S] + (C_g(\nu'h) - 2\tau\cos\beta)Im[S']\}$$

$$+\frac{\rho\tau}{2}\iint_{S_F}(\psi - y)Im[\phi^1\frac{\partial^2\phi^*}{\partial z^2}]dS - \rho U\iint_{S_b}(\psi - y)V_n^2 dS$$

where

$$S = \sqrt{\frac{2\pi}{\nu}} e^{\frac{i\pi}{4}} H^*(\beta + 2\frac{\tau}{C_g(\nu'h)} sin\beta)$$

H is similar to the Kochin funtion but includes the free surface integral. ψ denotes the steady potential corrensponding to sway mode and V_n^2 denotes the 2nd-order component of the normal velocity due to the linear body motion without forward speed.

4 Wave drift damping

F_x may be expanded in the form

$$F_x = F_{x0} + FrF_{x1}$$

where F_{x1} is the wave drift damping.

$$\Phi = \phi_s(x) + Re(\phi(x)e^{i\sigma t}) + \psi(x) + ...$$

Estimation of the accuracy of $\frac{\partial G^0}{\partial K}$.

Current Participants

Chevron

ConocoPhillips

OTRC

Petrobras/USP

Shell

StatoilHydro

Rolf Baarholm
Statoil ASA
Arkitekt Ebbels veg 10
Rotvoll, Trondheim
Norway
rolbaa@statoil.com

Marcos Ferreira
Petrobras SA
Eng. Marcos Donato Ferreira
CENPES/PDP/MC
Av Horacio Macedo, 950
Cidade Universitaria, Ilha do Fundao
21941-915
Rio de Janeiro, Brazil
marcos.donato@petrobras.com.br

Chang-Ho Lee
WAMIT
822 Boylston Street, Suite 202
Chestnut Hill, MA 02467
chlee@wamit.com

Stergios Liapis
Shell Oil Company
Offshore Structures
3737 Bellaire Blvd.
Houston, TX 77025
Phone) 713 245 7677
stergios.liapis@Shell.Com

Nick Newman
WAMIT
1 Bowditch Road
Woods Hole, MA 02543
jnn@mit.edu

John Niedzwecki
Offshore Technology Research Center
1200 Mariner Drive
College Station, TX 77845-3400
j-niedzwecki@tamu.edu

Robert Page
AeroHydro
54 Herrick Road/PO Box 684
Southwest Harbor, ME 04679-0684
robertpage@aerohydro.com

Amal C. Phadke
ConocoPhillips Company
600 N Dairy Ashford Rd, Office MO-01-1022
Houston, TX 77079
amal.c.phadke@conocophillips.com

Joao Sparano
University of Sao Paulo
Numerical Offshore Tank
Department of Naval Architecture and Ocean Engineering
Av. Prof. Mello Moraes, 2231
Cidade Universitaria
Sao Paulo, SP, Brazil CEPO05508-900
5511 3091-1704 ext. 250
sparano@usp.br

Xuemei Zhu
WAMIT Inc.
17 Berch Ct.
Wilton, CT 06897
xmzhu@wamit.com

Donald Danmeier
Chevron Energy Technology Co.
6001 Bollinger Canyon Road
Room L-4220
San Ramon, CA 94583-2324
DDanmeier@chevron.com

Rick Mercier
Offshore Technology Research Center
1200 Mariner Drive
College Station, TX 77845-3400
rmercier@civil.tamu.edu

Chad Petrash
ConocoPhillips Company
600 N Dairy Ashford Rd
Houston, TX 77079
chad.petrach@conocophillips.com

Per Teigen
StatoilHydro
Postuttak
N 7005 Trondheim
Norway
pte@statoilhydro.com

Street Address
Ark, Ebbels v.10
Rotvoll
Trondheim, Norway

John Letcher
AeroHydro
54 Herrick Road/PO Box 684
Southwest Harbor, ME 04679-0684
jletcher@aerohydro.com

Rune Yttervik
StatoilHydro ASA
Research Centre, Bergen
Norway
Rune.Yttervik@statoilhydro.com

Tim Finnigan
Chevron Energy Technology Co.
6001 Bollinger Canyon Road
Room L-4296
San Ramon, CA 94583-2324
TimFinnigan@Chevron.com

Finn Gunnar Nielsen
StatoilHydro ASA
PO Box 7190
N-5020 Bergen, Norway
Finn.Gunnar.Nielsen@statoilhydro.com

Street Address
Sandsliveien 90
N-5254 Sandsli, Norway

Kazuo Nishimoto
Kazuo Nishimoto, Prof. Dr.
Department of Naval Architecture & Ocean Engineering
EPUSP
Numerical Offshore Tank - TPN
Av. Prof. Mello Moraes, 2231, Cidade Universitária
CEP05508-900, SP, SP, Brazil
knishimo@usp.br

Michael Shook
AeroHydro
54 Herrick Road/PO Box 684
Southwest Harbor, ME 04679-0684

mshook@aerohydro.com

George Gu
ConocoPhillips
MO-01-1020
600 North Dairy Ashford
Houston, TX 77079
george.z.gu@conocophillips.com